Soils and Foundations 63 (2023) 101328 https://doi.org/10.1016/j.sandf.2023.101328

On the modelling of stress-dilatancy behavior in weakly cemented sands

Saurabh Singh, Ramesh Kannan Kandasami, Tejas G. Murthy, Matthew Richard Coop

[Outline]

Understanding & modeling of stress-dilatancy behavior of weakly cemented sands

Constitutive models have focused on clean sand and soft clays

↕

cemented sands, which exhibit both soil and rock characteristics

{require modified models that account for inter-particle cohesion and bond strength}

[Methods]

Monotonic drained triaxial compression tests

{cemented specimens} ↔ {uncemented sand specimens}

Evaluate effectiveness of using equivalent confining pressure to inter-particle cohesion.

Examine the stress-dilatancy response by applying different confining pressures

[Results]

Initial stiffness of cement sand was comparable to equivalent sand at low confining pressures

However, peak strength and dilation were significantly higher in cemented sand.

Stress-dilatancy response of cement sand converge to that of and at high confining pressure

Cemented sand exhibited a dilatancy ratio significantly affected by the cement content and relative density.

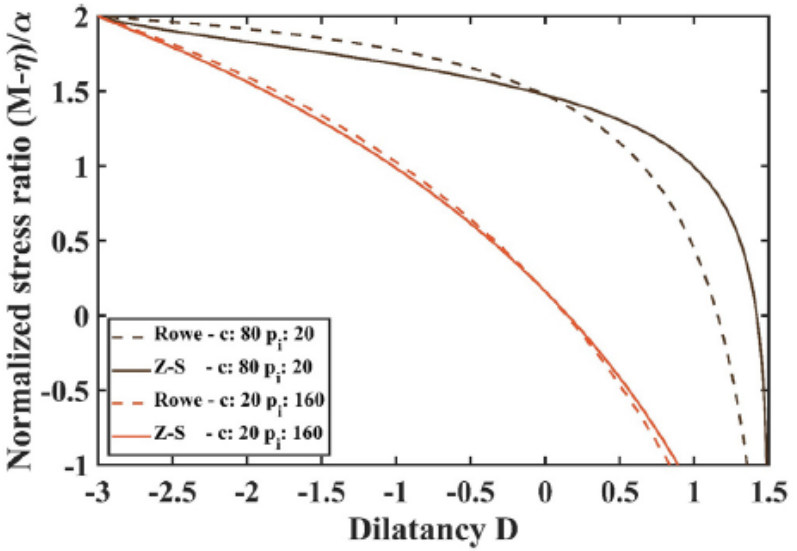

Fig. 9. Stress-dilatancy relations for cemented sand and equivalent sand.

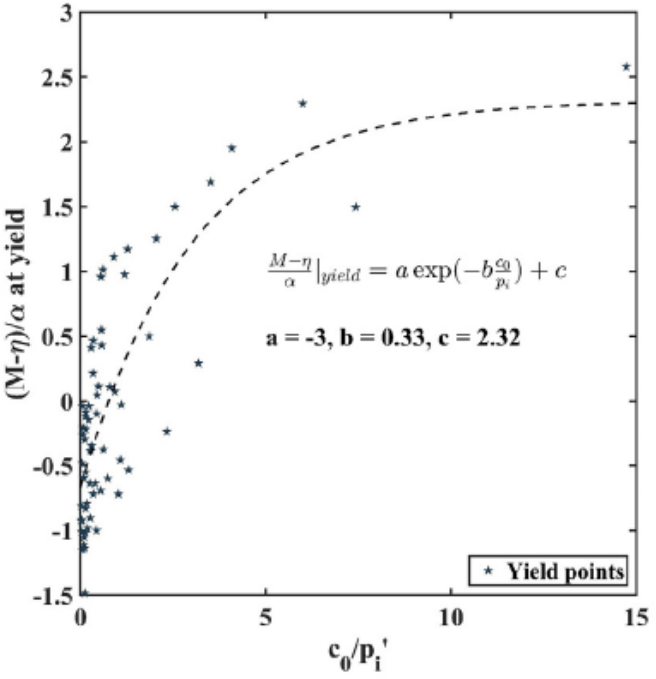

(c) Yield locus

Soils and Foundations 63 (2023) 101357 https://doi.org/10.1016/j.sandf.2023.101357

Shaking table test on underwater slope failure induced by liquefaction

Xiaoqing Feng, Bin Ye, Jie He, Husheng Miao, Chuangji Lin

[Outline] Large deformation of flow liquefaction in the loose sediment region (underwater slope failure)
Dynamic response characteristics of liquefaction in underwater slopes is required
→ Shaking table tests to simulate and analyze the entire process of liquefaction-induced slope failure.

[Methods] Underwater sand slope model. PIV, measuring acc and EPWP
Shaking table tests (acc amplitude, frequency, relative density, slope ratio)

[Results] higher accelerations → EPWP ratio
Higher frequencies → larger and quicker peaks in EPWP ratio
Lower relative density → led to more pronounced liquefaction
Gentler slope ratios (1:1.93) were more prone to liquefaction compared to steeper slopes (1:1.14)
Acc > slope gradient > Dr > frequency

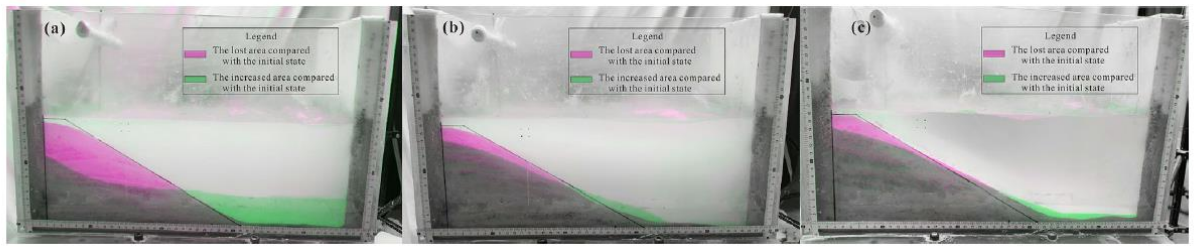

Fig. 10. Comparison between the initial state and the final state of the slope for various acceleration amplitudes with the slope ratio of 1:1.93, the frequency of 4 Hz, and the relative density of 32.9%: (a) 0.32 g (b) 0.22 g (c) 0.16 g.

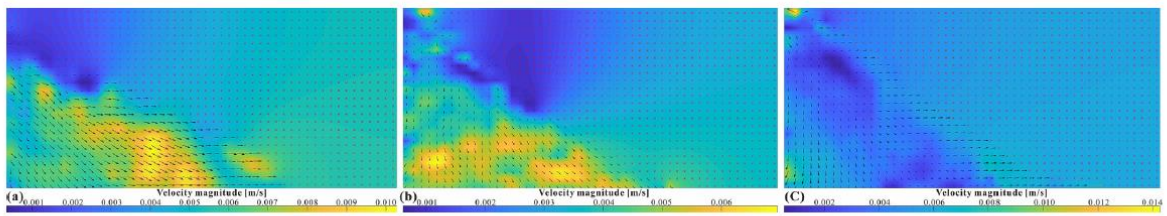

Fig. 11. PIV vector results at the same time for various acceleration amplitudes with the slope ratio of 1:1.93, the frequency of 4 Hz, and the relative density of 32.9%: (a) 0.32 g (b) 0.22 g (c) 0.16 g.

Soils and Foundations 63 (2023) 101338 https://doi.org/10.1016/j.sandf.2023.101338

SPH approach for stability analysis of soil slope with variable permeabilities

Binghui Cui, Liaojun Zhang, Weiqiang Wang, Yifei Sun

[Outline]

Soil–water interaction (post-failure/progressive of slopes by liquefaction)

Failure mechanisms and hazard characteristics; SPH

Large deformations affects the changes in density and permeability.

→ changes is the dilatation tendency of the soil in shear deformation.

Biot's; changes in pore water pressure caused by large deformations are transient (negligible).

limited research on changes in soil permeability within SPH by modifying to simulate large soil slope deformations

[Methods]

Two-phase model within SPH through drag forces based on Darcy's law.

Changes in soil porosity and permeability were automatically adjusted

[Results]

Sliding distance differed by about 10% between cases with and without considering changes in permeability

Initial porosity was found to have substantial negative effect

Variable permeabilities have a slight effect on overall slope stability but significantly impact the sliding distance.

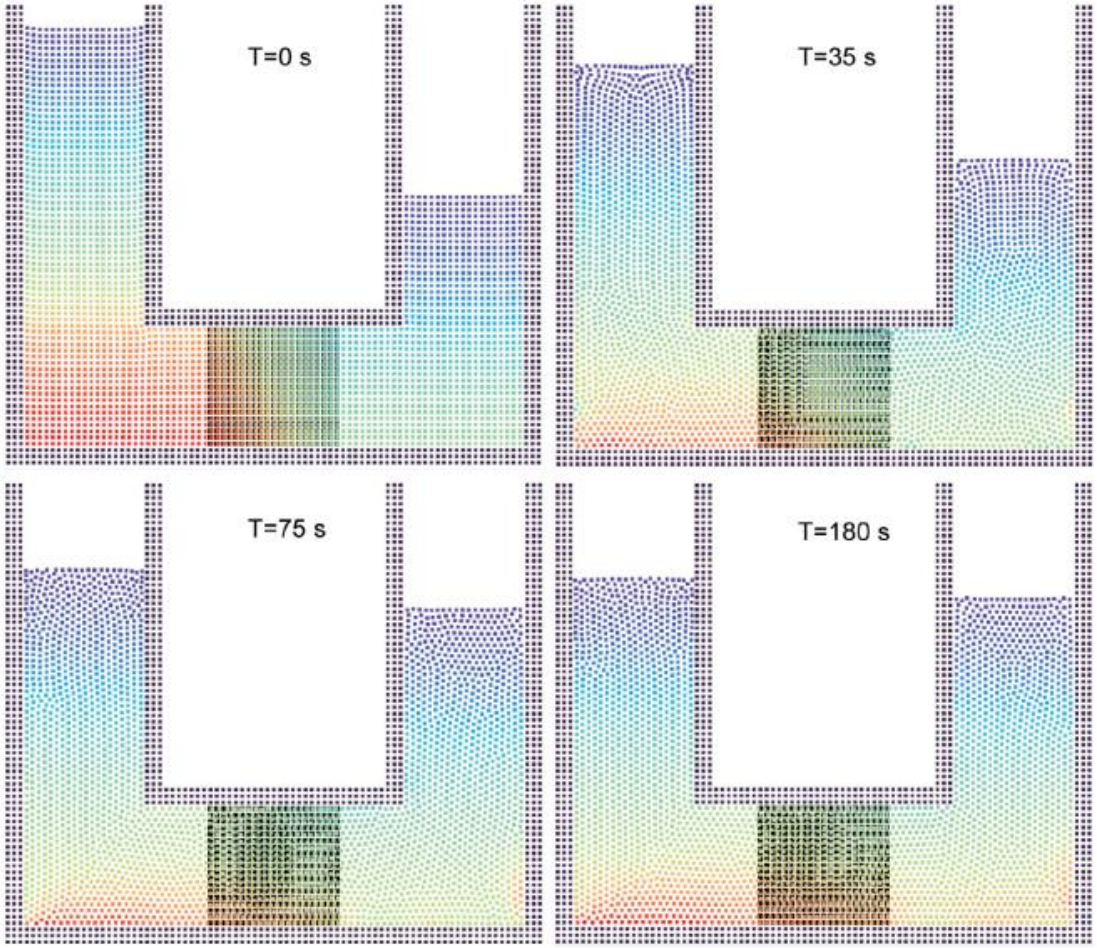

Fig. 4. Simulation of the U-tube seepage model at different times (k = 0.01).

Soils and Foundations 63 (2023) 101333 https://doi.org/10.1016/j.sandf.2023.101333

Treatment of cadmium-contaminated soil using ladle slag with and without CO2

Bo Xu, Anand J. Puppala, Yaolin Yi

[Outline]

Ordinary Portland cement (OPC) and lime stabilize/solidify cadmium-contaminated soils
↔ CO2 emissions and energy consumption.

Methods of using industrial by-product, ladle slag (LS), combined with CO2, to treat cadmium-contaminated soils

[Methods]

Laboratory tests on contaminated with cadmium at varying initial concentrations, treated with 10% binder content of LS, and subjected to standard and carbonation curing processes.

Treatment efficacy evaluation: unconfined compressive strength (UCS) tests and leaching tests of the treated soils.

Various chemical and micro-analyses

[Results] Research findings

Standard curing with LS was less effective than OPC in reducing cadmium leaching over a 28-day period

CO2 introduced carbonation curing improved effectiveness.

Carbonation curing with LS sequestered up to 16% of its mass in CO2 and resulted in higher strength than CO2 treated.

CO2 sequestration was most effective at an initial water content of 8%

higher initial concentrations of cadmium promoted carbonation reactions.

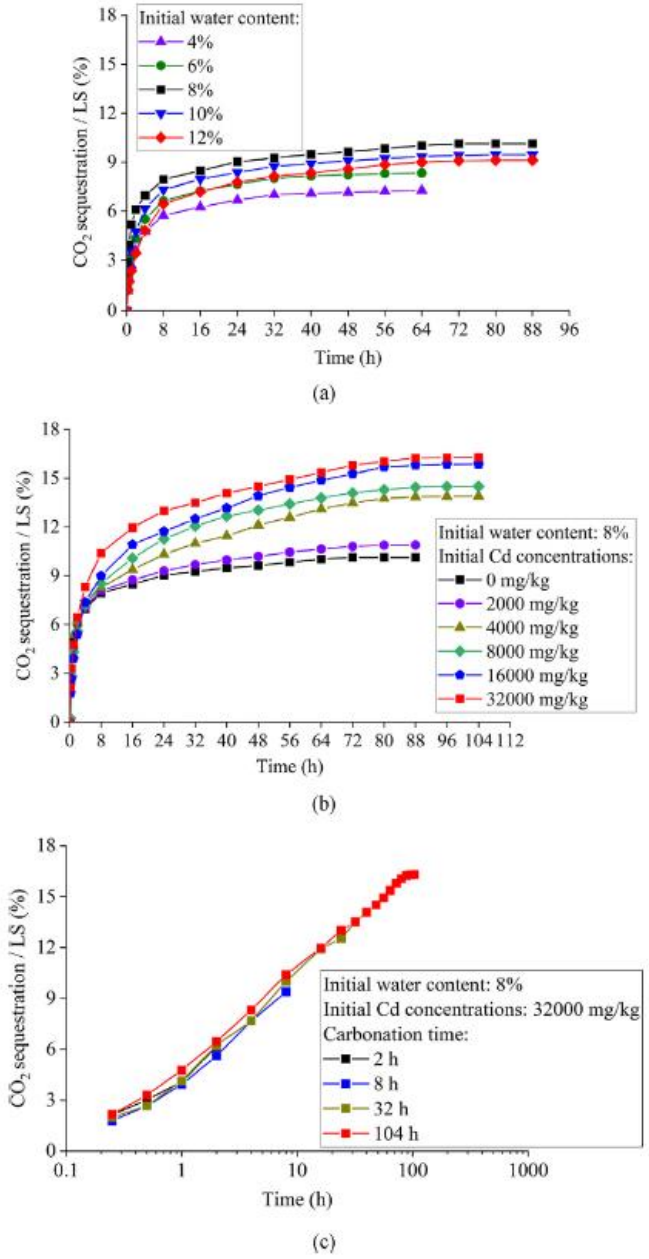

Fig. 3. CO_2 sequestration/LS with different (a) initial water contents, (b) initial concentrations of Cd, and (c) carbonation times.

Soils and Foundations 63 (2023) 101337 https://doi.org/10.1016/j.sandf.2023.101337

Uncertainty analysis for drilled shaft axial behavior using CYCU/DrilledShaft/143

Yit-Jin Chen, Kok-Kwang Phoon, Anjerick Topacio, Suneelkumar Laveti

[Outline]

Drilled shafts – transferring superstructure loads into ground.

These have uncertainties (variations in soil strength, anomalies during drilling)

These uncertainties necessitate reliable testing and modeling techniques to predict the actual behavior.

[Methods]

Use load test database (CYCU/DrilledShaft/143), including 143 drilled shaft tests under both drained and undrained conditions.

Normalization techniques and statistical analyses – to compare different interpretation criteria

[Results]

Variability in interpreted shaft capacities, depending on the criterion used.

(Chin method often predicted capacities higher than other methods, exceeding standard predictions by up to 30%)

Normalized load-displacement curves were fitted to a hyperbolic model

More conservative approach to estimating shaft capacity in varied soil conditions.

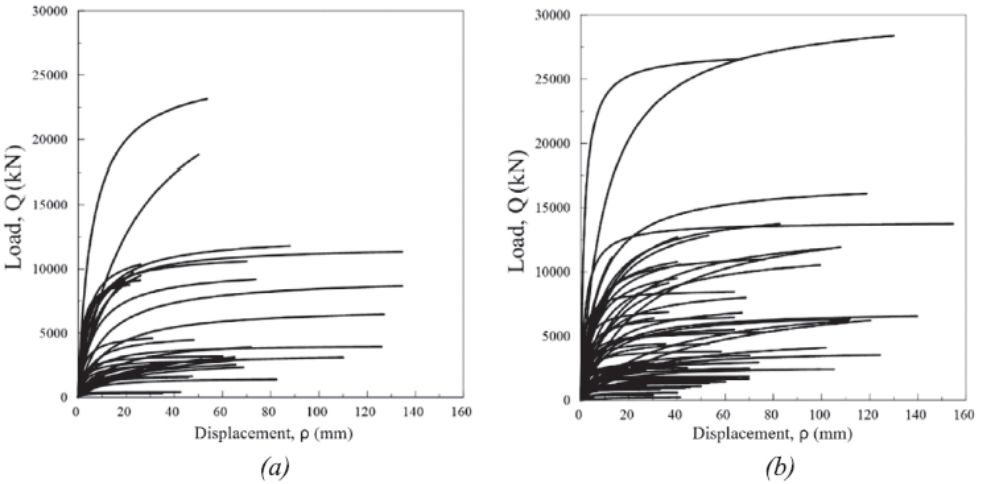

Fig. 5. Measured load–displacement curves for (a) drained (n = 61) and (b) undrained soil conditions (n = 82).

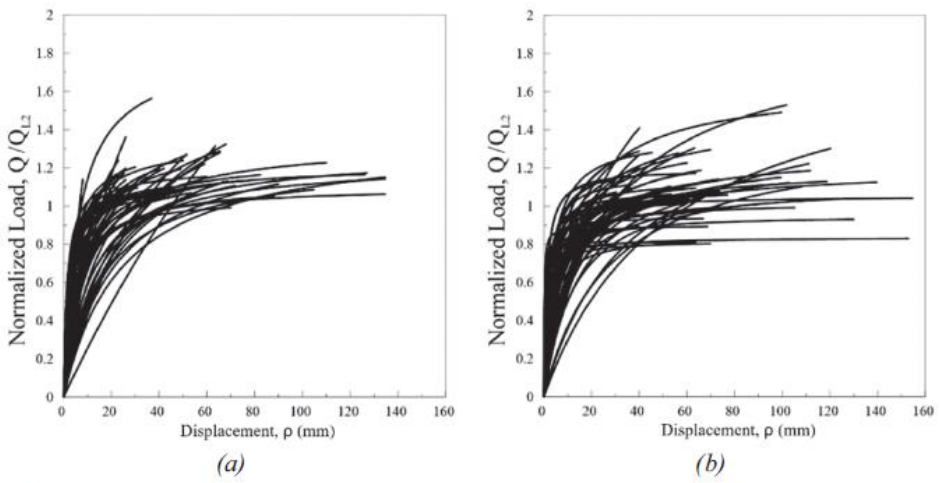

Fig. 6. Normalized load (Q/Q_{L2}) and displacement curves for (a) drained (n = 46) and (b) undrained soil conditions (n = 52).

Soils and Foundations 63 (2023) 101350 https://doi.org/10.1016/j.sandf.2023.101350

Water and soil particle movement in unsaturated bentonite with constrained and free swelling boundaries

Hailong Wang, Yuka Yamamoto, Hiroyuki Kyokawa, Daichi Ito, Hideo Komine

[Outline]

Bentonite – barrier material in geological disposal of radioactive waste

Understand of its behavior under wetting conditions (water absorption)

Water and soil particle movement in compacted bentonite during the wetting process

[Methods]

Experimental and numerical analyses under 2 boundary conditions: constrained and free swelling.

Gravimetric *w* was measured in bentonite specimens with varying dry densities, and water diffusivity (Dw) and soil particle diffusivity (Ds) were calculated.

[Results]

In constrained swelling, it was found that water diffusivity decreased with an increase in dry density.

Under free swelling conditions, measurements showed more dynamic and varied patterns of water and soil particle distribution, influenced by the initial dry density and swelling potential.

Numerical simulations shows the experimental outcomes, demonstrating the accuracy of the models in predicting water and soil behaviors in bentonite.

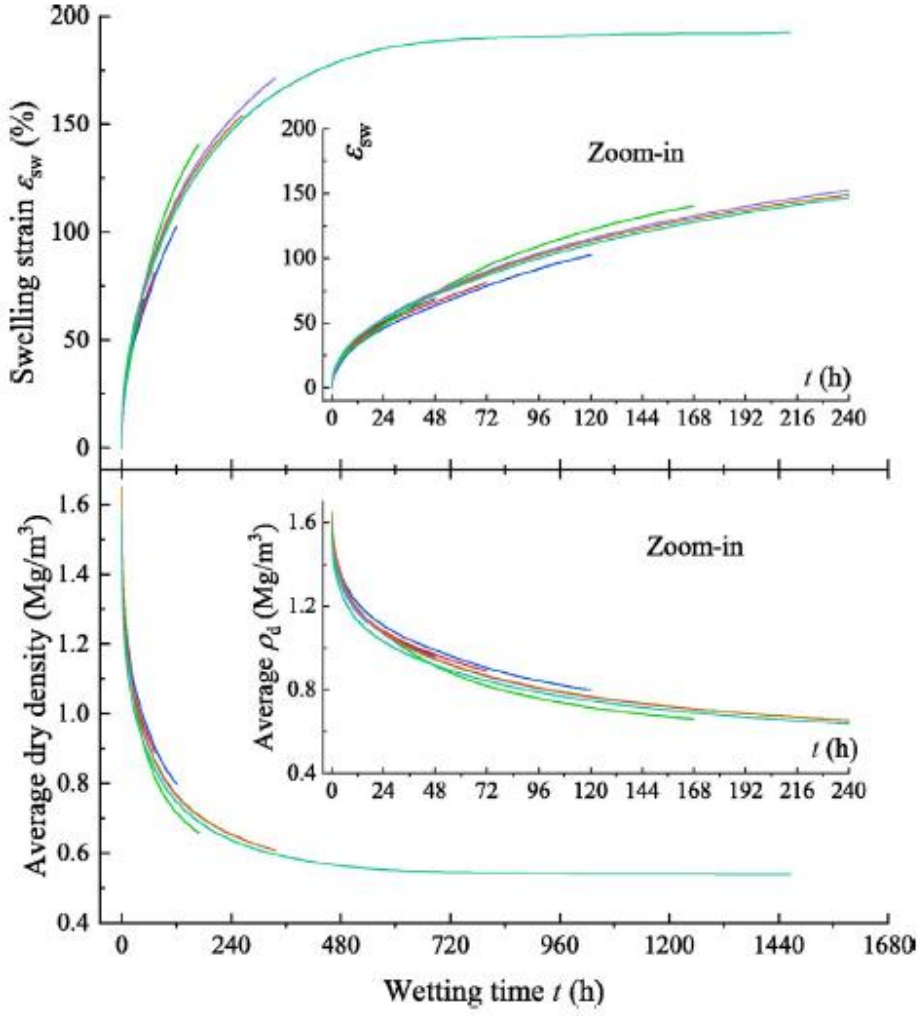

Fig. 4. Time histories of swelling strain and average dry density from free swelling tests.